Molecular Plant • Volume 4 • Number 5 • Pages 896–908 • September 2011 RESEARCH ARTICLE

Live-Cell Imaging of Dual-Labeled Golgi Stacks in Tobacco BY-2 Cells Reveals Similar Behaviors for Different Cisternae during Movement and Brefeldin A Treatment

Stephanie L. Madison and **Andreas Nebenführ**[1]

Department of Biochemistry and Cellular and Molecular Biology, University of Tennessee, Knoxville, TN 37996–0840, USA

ABSTRACT In plant cells, the Golgi apparatus consists of numerous stacks that, in turn, are composed of several flattened cisternae with a clear *cis*-to-*trans* polarity. During normal functioning within living cells, this unusual organelle displays a wide range of dynamic behaviors such as whole stack motility, constant membrane flux through the cisternae, and Golgi enzyme recycling through the ER. In order to further investigate various aspects of Golgi stack dynamics and integrity, we co-expressed pairs of established Golgi markers in tobacco BY-2 cells to distinguish sub-compartments of the Golgi during monensin treatments, movement, and brefeldin A (BFA)-induced disassembly. A combination of *cis* and *trans* markers revealed that Golgi stacks remain intact as they move through the cytoplasm. The Golgi stack orientation during these movements showed a slight preference for the *cis* side moving ahead, but *trans* cisternae were also found at the leading edge. During BFA treatments, the different sub-compartments of about half of the observed stacks fused with the ER sequentially; however, no consistent order could be detected. In contrast, the ionophore monensin resulted in swelling of *trans* cisternae while medial and particularly *cis* cisternae were mostly unaffected. Our results thus demonstrate a remarkable equivalence of the different cisternae with respect to movement and BFA-induced fusion with the ER. In addition, we propose that a combination of dual-label fluorescence microscopy and drug treatments can provide a simple alternative approach to the determination of protein localization to specific Golgi sub-compartments.

Key words: Golgi apparatus; Golgi stack integrity; brefeldin A; monensin; tobacco BY-2 cells; live-cell imaging.

INTRODUCTION

The Golgi apparatus is at the heart of the secretory system in both animal and plant cells. It consists of stacks of flattened membrane cisternae surrounded by vesicles and has a characteristic *cis*-to-*trans* polarity (reviewed in Staehelin and Moore, 1995; Polishchuk and Mironov, 2004; Staehelin and Kang, 2008). The Golgi apparatus is responsible for modifying and sorting proteins as well as synthesizing lipids. It plays a crucial role in the processing of N-linked glycans on glycoproteins, which is achieved by multiple glycosidases and glycosyltransferases that are arranged from the *cis* to the *trans* cisternae in the order in which they operate on their substrates (reviewed in de Graffenried and Bertozzi, 2004; Schoberer and Strasser, 2011). In plants, the Golgi apparatus also produces complex poly-saccharides needed for cell wall synthesis (Driouich et al., 1993). Only a few of the many enzymes predicted to be involved in the synthesis of pectins and hemicelluloses have been isolated to date and their localization within the different cisternae is just beginning to be unraveled (Chevalier et al., 2010). The *cis*-to-*trans* polarity of Golgi cisternae is also reflected in a progressive acidification of the cisternal lumen (Boss et al., 1984). This progressive drop in pH presumably plays a role in sorting of cargo molecules as well as activation of proteolytic enzymes in later Golgi compartments (Jiang and Rogers, 1999). Drugs, such as the cation ionophore monensin, that disrupt the pH gradient across the membrane therefore block secretion and lead to a swelling of the *trans* Golgi network (TGN) and *trans* cisternae (Zhang et al., 1992).

[1] To whom correspondence should be addressed. E-mail nebenfuehr@utk.edu, tel. +1-865-974-9201, fax +1-875-974-6306.

doi: 10.1093/mp/ssr067, Advance Access publication 25 August 2011
Received 4 May 2011; accepted 12 July 2011

A unique characteristic of the plant Golgi apparatus is that it consists of numerous motile stacks (Boevink et al., 1998; Nebenführ et al., 1999). These stacks are approximately 300 nm thick with a cisternal diameter ~800 nm. Plant Golgi stack movements are dependent on the actin cytoskeleton and myosin motor proteins (Nebenführ et al., 1999; Avisar et al., 2008; Peremyslov et al., 2008). Even though Golgi stack motility in plants has been observed for over a decade, there are still unanswered questions surrounding the underlying mechanisms. First, it is not known how myosin motors mediate Golgi movements. It is possible that myosin motors could attach directly to Golgi stacks (Li and Nebenführ, 2007) and thus move them in parallel to but essentially independently of the actin-associated ER network. Alternatively, Golgi stacks could move through the cell by attaching to endoplasmic reticulum export sites (ERES), which, in turn, are part of the motile ER (Runions et al., 2006; Ueda et al., 2010). Second, we have only a very general understanding of how Golgi stack integrity is maintained in the face of the physical shear forces that are likely to act upon stacks during their movement through the cytoplasm. The matrix proteins that surround Golgi cisternae are currently the best candidates for providing the cohesive forces that maintain cisternal association (Latijnhouwers et al., 2005; Renna et al., 2005; Latijnhouwers et al., 2007; Matheson et al., 2007), although the specific interactions that mediate Golgi stack integrity are still unknown.

The structural organization of the Golgi apparatus into cisternae of different protein compositions is dynamically maintained by a complex interplay of anterograde and retrograde transport mechanisms. The anterograde flow of cargo through Golgi stacks is most likely mediated by a cisternal progression/maturation mechanism whereby individual cisternae are being pushed through the stack while their membrane composition is continuously modified by recycling Golgi-resident enzymes back to earlier compartments (Nebenführ, 2003; Schoberer and Strasser, 2011). This retrograde transport has been shown to depend on COPI vesicles (Letourneur et al., 1994). Interestingly, Golgi enzyme recycling reaches as far back as the ER (Brandizzi et al., 2002) so that Golgi stack maintenance also depends on continuous export from the ER. Indeed, Golgi stacks can be disrupted and Golgi enzymes redistributed to the ER by overexpressing a GTP-locked form of Sar1, the small GTPase necessary for COPII vesicle formation at ERES (Osterrieder et al., 2010; Schoberer et al., 2010).

Curiously, inhibition of the COPI-dependent retrograde recycling pathway with the fungal drug brefeldin A (BFA) also leads to a redistribution of Golgi enzymes into the ER (Boevink et al., 1998; Lee et al., 2002; Ritzenthaler et al., 2002; Saint-Jore et al., 2002; Schoberer et al., 2010). This redistribution most likely depends on direct membrane continuities between Golgi cisternae and the ER (Sciaky et al., 1997; Ritzenthaler et al., 2002), although the mechanism by which these continuities occur is still debated. One model posits that loss of COPI coats during BFA treatment exposes SNARE proteins on the cisternal surface that normally mediate fusion of Golgi-derived vesicles with the ER (Elazar et al., 1994; Nebenführ et al., 2002; Ritzenthaler et al., 2002). Another model assumes that such COPI-independent membrane continuities occur also under normal conditions to mediate recycling of Golgi residents (Schoberer et al., 2010). Interestingly, two independent studies have concluded that the disassembly of Golgi stacks during BFA treatments occurs directionally such that *trans* cisternae fuse with the ER first, while *cis* cisternae fuse last (Ritzenthaler et al., 2002; Schoberer et al., 2010). While the first study was mostly based on the analysis of EM images taken at various time points during the BFA treatment (Ritzenthaler et al., 2002), the second study relied on the observation of fluorescent markers that localized to different Golgi subcompartments as well as fluorescently labeled Golgi matrix proteins (Schoberer et al., 2010).

In this study, we revisit these questions in tobacco BY-2 suspension-cultured cells that carry dual-labeled Golgi stacks. We present detailed time-lapse observations of individual Golgi stacks during normal movement as well as during BFA and monensin treatments. Our results reveal both a remarkable stability of Golgi stacks as well as an unexpected equivalence of the *cis* and *trans* sides.

RESULTS

Dual-Labeled Golgi Stacks Reveal Different Localization of Marker Proteins

To examine Golgi stack movements and disassembly, fluorescent proteins were fused to the transmembrane domains of Golgi proteins that have been shown to localize to different cisternae with various degrees of overlap. As a *cis* marker, we used a full-length clone of soybean α-1,2 mannosidase I fused to YFP (ManI–YFP; Nebenführ et al., 1999). We also utilized a medial marker that consists of the first 36 amino acids of *Arabidopsis thaliana* β1,2-xylosyltransferase fused with YFP (XT–YFP; Pagny et al., 2003). Finally, we employed the first 52 amino acids of rat α-2,6-sialyltransferase fused to YFP or CFP (ST–YFP/ST–CFP), which primarily localizes to the *trans* half of the Golgi (Boevink et al., 1998).

Pairs of fusion proteins were examined in the cortical cytoplasm after stable co-expression in tobacco BY-2 cells. Golgi stacks in cell lines expressing either ManI–YFP and ST–CFP or XT–YFP and ST–CFP often appeared tri-colored due to partial overlap (Figure 1A, 1B, 1D, and 1E). This is most noticeable in the side-views shown in the insets of Figure 1D and 1E. There appeared to be more non-overlapping regions when ST–CFP was co-expressed with ManI–YFP than with XT–YFP. This was confirmed by determining the centers of the labeled cisternae with a peak-finding algorithm. This analysis revealed that ST–CFP cisternae were, on average, slightly closer to XT–YFP cisternae (0.20 ± 0.01 μm; SE, n = 115 from four cells) than to ManI–YFP cisternae (0.21 ± 0.01 μm; SE, n = 125 from eight cells), although this difference was not statistically significant (Mann-Whitney test, $p > 0.05$). Thus, our observations support previous findings that these proteins localize to different

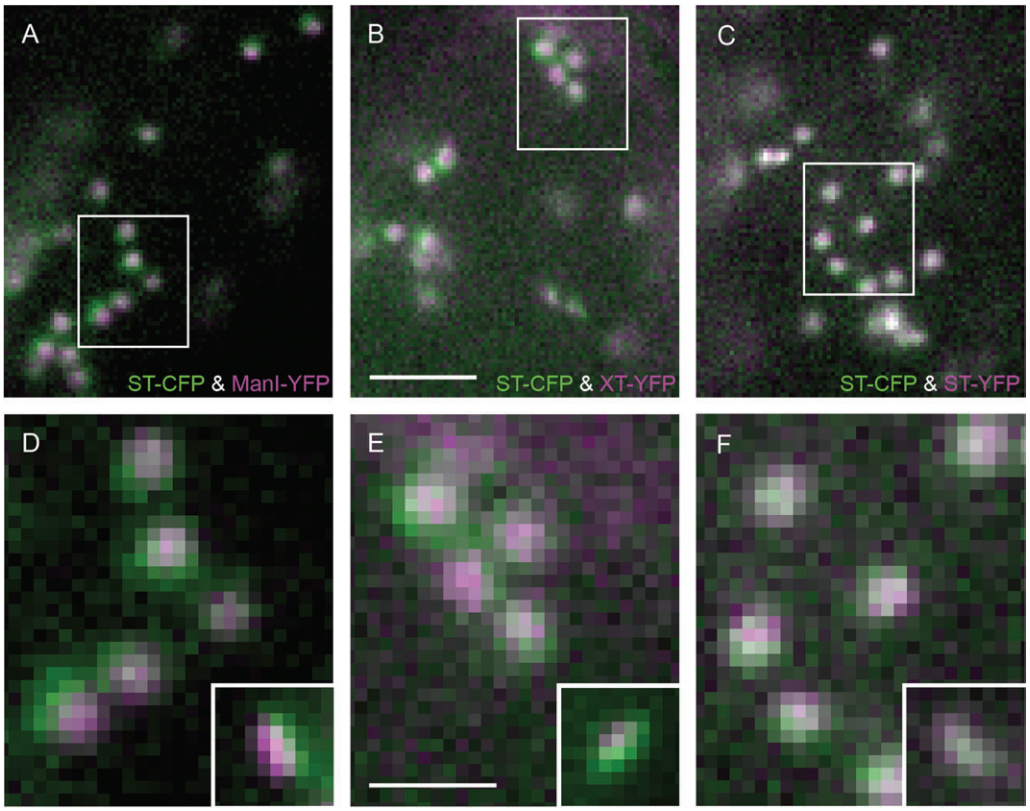

Figure 1. Differential Localization of Marker Proteins in Dual-Labeled Golgi Stacks.

Transgenic tobacco BY-2 cells co-expressing ST–CFP **(A–F)** and ManI–YFP (A, D), XT–YFP (B, E), or ST–YFP (C, F). Outlined regions in (A–C) are magnified 3× in (D–F). Note the different degrees of overlap between the ST–CFP (green) and the YFP fusions (magenta). The region of overlap (white) is most notable in the side-views shown for different stacks at the same magnification in the insets (D–F). ST–CFP and ST–YFP are almost completely overlapped while ST–CFP and XT–YFP and ST–CFP and ManI–YFP have a smaller overlapping region. Scale bar = 5 μm in (A–C) and 2 μm in (D–F).

cisternae (Boevink et al., 1998; Nebenführ et al., 1999; Pagny et al., 2003). In contrast, Golgi stacks in cell lines expressing ST–YFP and ST–CFP usually appeared predominantly white with no clear separation between the channels because both fusion proteins localized to the *trans* cisternae (Figure 1C, 1F). Consistent with this impression, the average distance between ST–CFP and ST–YFP cisternae was only about half a pixel (0.09 ± 0.01 μm; SE, n = 137 from five cells). This slight displacement may have been caused by the temporal delay between CFP and YFP image capture, or could simply reflect random noise.

Monensin Treatment Affects *Trans* Cisternae More than *Cis* and Medial Cisternae

Previous studies have shown that treating plant cells with monensin, an ionophore that is specific for monovalent cations, ultimately results in the sequential swelling of Golgi cisternae (Zhang et al., 1992), presumably due to the resulting influx into acidic late Golgi compartments (Zhang et al., 1992; Satiat-Jeunemaitre et al., 1994). In the electron micrographs, it could be observed that the *trans* Golgi network is the first to swell followed by the *trans* cisternae. Medial and *cis* cisternae started to swell only later during the treatment.

The rate of swelling of different cisternae was observed by live-cell imaging in BY-2 cells co-expressing ST–CFP and ManI–YFP (Figure 2A) or XT–YFP (Figure 2B). Cells were treated with 10 μM monensin and 1 μM latrunculin B (to prevent movement of the stacks) and observed using sequential time-lapse imaging with 10-s intervals between images. In cells expressing either ST–CFP and ManI–YFP or ST–CFP and XT–YFP, the cisternae labeled with ST–CFP began to swell by 5 min and appeared to reach a maximum size by 35 min after the addition of monensin (Figure 2 and Supplemental Movies 1 and 2). Swelling of the *cis* and medial cisternae was less noticeable, but these cisternae appeared to start enlarging by about 30 min after the start of the monensin treatment. Quantitative analysis of the apparent cisternal sizes at 0 and 50 min in monensin confirmed these impressions and revealed that *trans* cisternae swelled on average by ~50% whereas medial and *cis* cisternae increased in size by only ~20 and ~10%, respectively (n = 12–30 in two cells per treatment).

Frequently, we observed swollen cisternae containing the ST–CFP marker surrounded by smaller cisternae labeled with either the ManI–YFP or XT–YFP marker (Figure 2). In some cases, the swelling of the cisternae also coincided with an

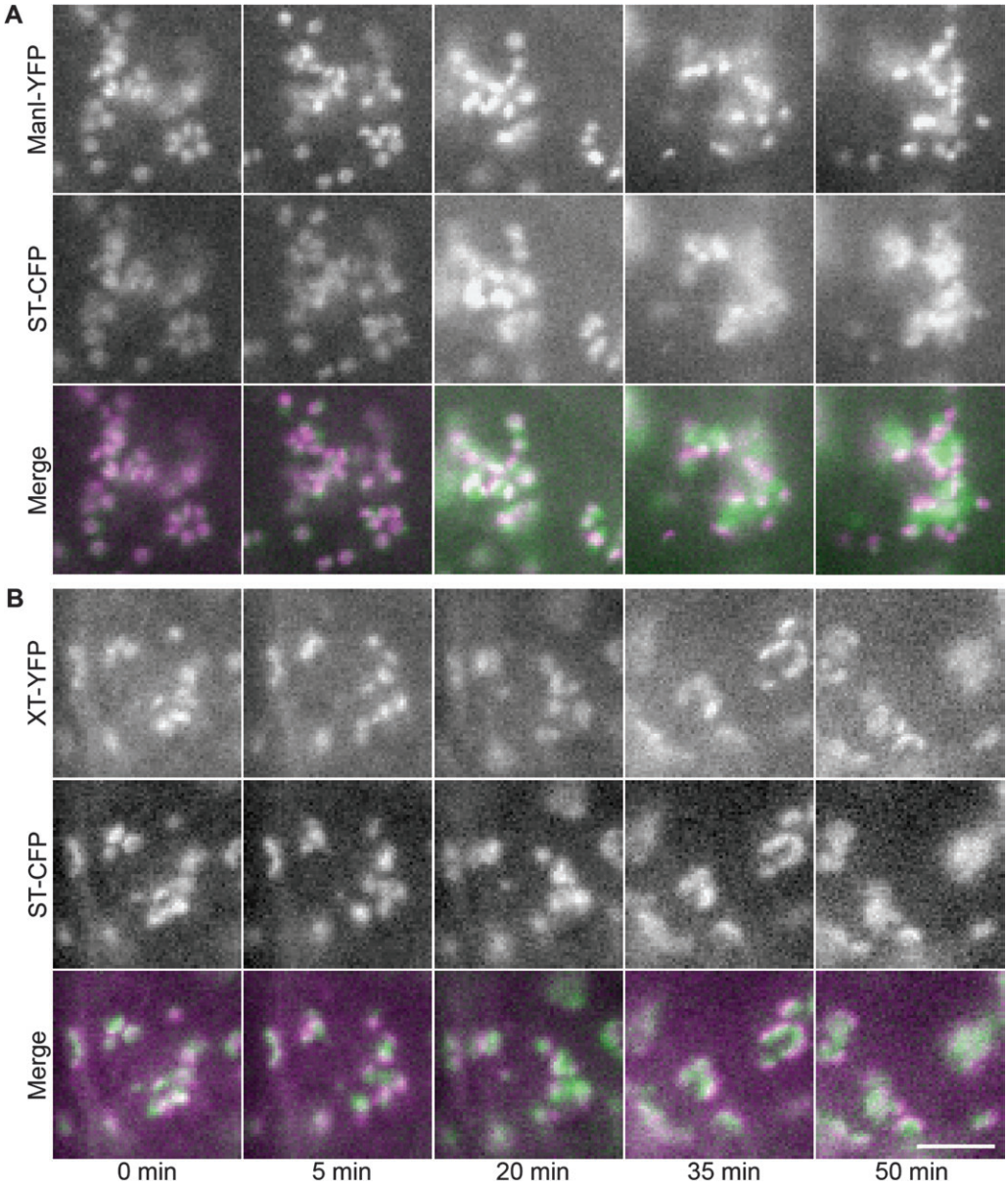

Figure 2. Monensin Treatment Preferentially Affects *Trans* Cisternae.

Transgenic tobacco BY-2 cells co-expressing ST–CFP (green) and ManI–YFP (magenta **(A)**) or XT–YFP (magenta **(B)**) were observed 0–50 min after addition of monensin. Note the increase in fluorescence intensity in (A) beginning at 20 min. Also, note that the *trans* cisternae swelled to a greater extent than the *cis* and medial cisternae. Due to the focus shifting during the time lapse, different stacks are shown after 20 min. Scale bar = 5 μm.

increase in fluorescence intensities. This increase is clearly visible in Figure 2A (20–50 min). Confirming previous studies, the *trans* cisternae were more affected by monensin treatment than the other cisternae.

Golgi Stacks Move as Intact Units with a Slight Preference for the *Cis* Cisternae to Lead

For over a decade, it has been known that plant Golgi stacks are motile and that their movements are dependent on the actomyosin network (Boevink et al., 1998; Nebenführ et al., 1999). While it is generally assumed that Golgi cisternae remain stacked during these movements, this has not been tested experimentally. Furthermore, it has yet to be determined whether Golgi stacks have a particular orientation while traveling through the cytoplasm.

To address these questions, we took advantage of the BY-2 suspension culture cell line that stably expressed ST–CFP and ManI–YFP. Simultaneous image capture of the two fluorophores was used to observe Golgi stacks at 1-s intervals for 1 min (Figure 3A and Supplemental Movie 3). Since there was no delay between the CFP and YFP images, it was possible

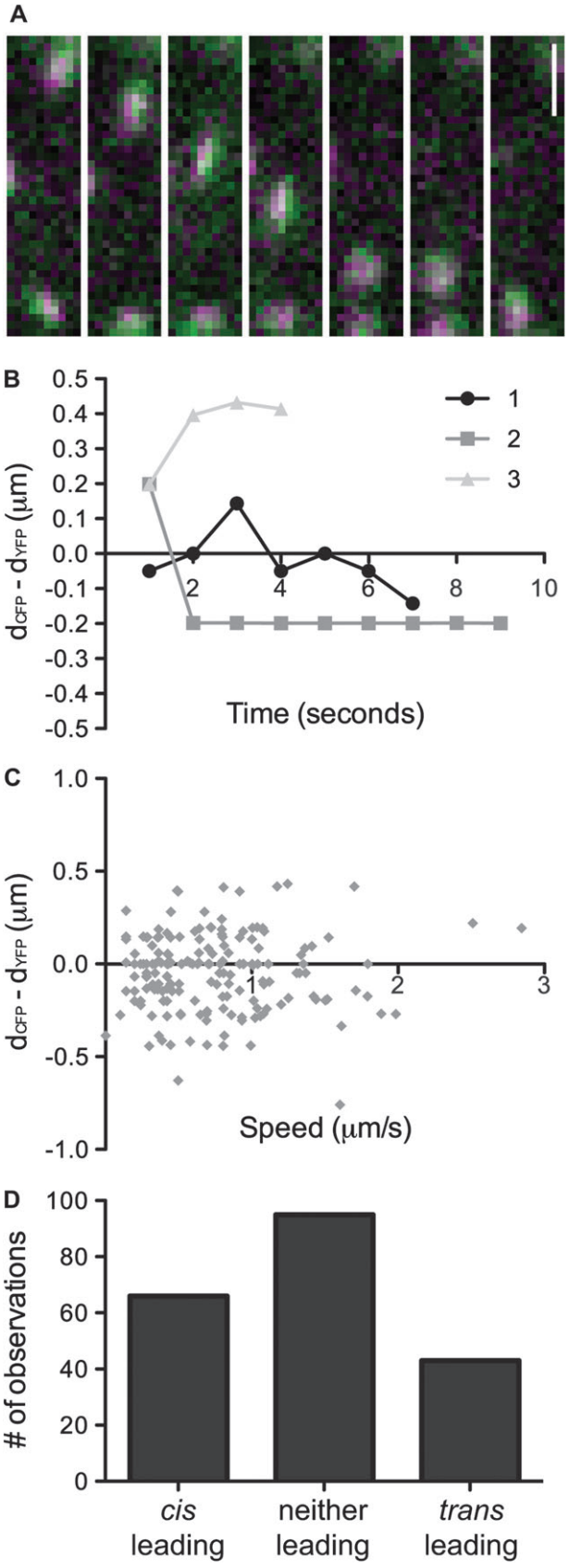

Figure 3. Golgi Stacks Move as Intact Units at Various Speeds and Orientations.

(A) Transgenic tobacco BY-2 cells co-expressing ST–CFP (green) and ManI–YFP (magenta) were imaged at 1-s intervals with simultaneous image capture for CFP and YFP channels. Scale bar = 2 μm.
(B) For each Golgi stack, the distance between the *trans* and *cis* cisternae ($d_{CFP} - d_{YFP}$) was calculated in every frame. Positive values indicate that the *trans* half was ahead, while negative values indicate that the *cis* half was ahead. Example 1 shows the distance between cisternae for the stack shown in (A). Note that stacks can have various orientations while moving.
(C) Instantaneous speeds were also calculated for every measurement of 20 different stacks. Note there is no correlation between speed and the distance between cisternae or stack orientation.
(D) Summary of Golgi stack orientation in individual frames. A cisterna was counted as leading if the distance between the markers was larger than 0.14 μm.

to calculate the distance between the *cis* and *trans* cisternae in any given frame. Movements of 20 individual Golgi stacks in the video sequences from eight cells were independently tracked in both the CFP and YFP images, and the distance between the two signals in the direction of movement was calculated ($d_{CFP} - d_{YFP}$). Positive distance values indicate that the *trans* end was moving ahead for a given frame, while negative values suggest that the *cis* half was leading at that time (Figure 3B). In all observed stacks, the *cis* and *trans* markers remained in close proximity during the movements (maximal distance between centers <0.8 μm), suggesting that Golgi stack integrity was maintained during movements. Of the 20 stacks observed, eight consistently had either the *trans* or *cis* cisternae leading (examples 2 and 3 in Figure 3B), while 12 stacks alternated which end was ahead during the time lapse (Figure 3A and example 1 in Figure 3B).

Since either half of the Golgi stack could lead during movements, we next asked whether there was a correlation between orientation and speed of the Golgi stack at different time points. Analysis of a total of 204 time points revealed that orientation of a Golgi stack during movement was not influenced by its speed (Figure 3C). Furthermore, there was also no correlation between the distance between cisternae and speed of the stack (Figure 3C). This suggests that Golgi stacks remain intact and do not show a preferential orientation while moving at speeds of 0–3 μm s^{-1}. This was further explored by comparing the number of cases in which the *cis* half, *trans* half, or neither half was leading (Figure 3D). Neither half was considered to be leading when the distance between the ST–CFP and ManI–YFP markers was less than 0.14 μm, which is one half of the diagonal of a pixel. Using this criterion, neither end of the observed stacks was clearly leading in almost half of the time points. In the remaining half of the observations, there was a slight but significant preference for the *cis* cisternae to lead while the stacks were moving (Figure 3D; $\chi^2 = 4.85$, $p = 0.028$).

Golgi Stack Disassembly Can Occur in Either the *Trans*-to-*Cis* or *Cis*-to-*Trans* Direction

Brefeldin A (BFA) treatment is known to cause the redistribution of Golgi enzymes to the endoplasmic reticulum (ER; Boevink

et al., 1998; Ritzenthaler et al., 2002; Saint-Jore et al., 2002; Schoberer et al., 2010). It has been proposed that this redistribution occurs sequentially, beginning with the *trans* cisternae and progressing to the *cis* (Ritzenthaler et al., 2002; Schoberer et al., 2010); however, this redistribution has not been observed for individual stacks as it is occurring. To re-examine the order of redistribution of Golgi enzymes, tobacco BY-2 cells co-expressing ManI–YFP and ST–CFP, XT–YFP and ST–CFP, or ST–YFP and ST–CFP, respectively, were treated with 10 μg ml^{-1} brefeldin A (36 μM BFA) and 1 μM latrunculin B (LatB). LatB stopped all Golgi movements (data not shown) and prevented the observed stacks from moving out of the focal plane, thus ensuring that changes in fluorescence intensity were only due to fusion with the ER. It is important to note that BFA-induced redistribution of Golgi enzymes to the ER is not dependent on cytoskeletal networks (Saint-Jore et al., 2002).

During the course of BFA treatment, the cells gradually lost distinct Golgi stacks (Figure 4A and Supplemental Movie 4) while, slowly, an ER-like network appeared (data not shown). This recapitulates results previously obtained by several groups (Boevink et al., 1998; Ritzenthaler et al., 2002; Saint-Jore et al., 2002; Schoberer et al., 2010).

To gain a more detailed view of the events during Golgi–ER fusion, tobacco BY-2 cells were observed during the first 20 min following the addition of BFA using time-lapse imaging (Figure 4A and Supplemental Movie 4). Images were taken in 5-s intervals and the CFP and YFP intensities of individual Golgi stacks were measured. Sometimes, multiple Golgi stacks were too close together to analyze separately; these clusters were measured as one unit as long as all included stacks responded to BFA at the same time. The maximal fluorescence intensities of individual stacks were plotted against the treatment time (Figure 4B–4E) and used to determine the timing of the loss of Golgi signal for each marker. Several different behaviors of the two markers were observed. Many stacks lost both markers simultaneously (Figure 4B and 4D). Others lost only the ST–CFP marker while ManI–YFP remained largely unchanged (Figure 4C). Still other Golgi stacks lost only the ManI–YFP marker (Figure 4E). Interestingly, we also observed Golgi stacks that lost one of their fluorescent markers in several steps, suggesting that these events could represent individual cisternae fusing with the ER (ManI–YFP in Figure 4B). In many cases, we observed a brief increase in fluorescence intensity immediately preceding the loss of a fluorescent marker from the Golgi stack (e.g. Figure 4B and 4D).

In those cases in which, initially, only one marker was lost from a Golgi stack, the other marker eventually also disappeared into the ER, thus leaving no trace of the Golgi stack (data not shown). The sequential loss of the two fluorescent markers could occur in close succession or with more delay. Depending on the relative timing of these events, we assigned them to one of five categories: those that lost both signals within less than 10 s of each other (CFP $\approx$ YFP), those where the two events occurred within 10–30 s of each other (CFP $>$ YFP and CFP $<$ YFP), and those events in which loss of one marker preceded loss of the other one by more than 30 s (CFP » YFP and CFP « YFP). When tobacco BY-2 cells co-expressing ManI–YFP and ST–CFP were treated with BFA, about half of the Golgi stacks lost both markers within 10 s of each other. The remaining half was split more or less evenly between those that lost the *trans* marker first (CFP $<$ YFP and CFP « YFP) and those that lost the *cis* marker first (CFP $>$ YFP and CFP » YFP). Therefore, fusion of *cis* and *trans* cisternae with the ER occurred more or less simultaneously for about half of the stacks, and the sequential cisternal loss of the other stacks did not show a preference for either *cis* or *trans* cisternae to fuse first with the ER (n = 103 from 14 cells; Figure 5A).

Similar results were obtained when tobacco BY-2 cells co-expressing XT–YFP and ST–CFP were treated with BFA (n = 65 from 13 cells; Figure 5A). In about half of the Golgi stacks observed, the YFP and CFP signals were lost simultaneously. The other stacks were distributed more or less evenly between those that lost the *trans* marker first (CFP $<$ YFP and CFP « YFP) and those that lost the medial marker first (CFP $>$ YFP and CFP » YFP). Interestingly, when the redistribution occurred sequentially, there was, on average, less of a delay between the medial and *trans* markers than between the *cis* and *trans* markers. In particular, the ratio of stacks that lost their markers sequentially within 30 s of each other (CFP $>$ YFP and CFP $<$ YFP) to those that lost their markers with a delay of more than 30 s (CFP » YFP and CFP « YFP) was 0.37 for the *cis*–*trans* marker pair and 1.83 for the medial–*trans* marker pair.

As a control, tobacco BY-2 cells co-expressing ST–YFP and ST–CFP were also treated with BFA. We did not expect to observe sequential fusion with the ER, since both markers were localized to the same compartment. In almost all of the Golgi stacks observed (n = 64 from 18 cells), YFP and CFP signals were lost simultaneously; however, two Golgi stacks showed loss of the CFP signal 10 s before the loss of the YFP signal. Thus, as expected, when YFP and CFP were both fused to the same Golgi protein, loss of both markers generally occurred simultaneously (Figure 5A).

The summary of Golgi stack behavior did not reveal a specific pattern for the sequential loss of cisternae (Figure 5A). However, it is possible that such patterns could have been masked by condensing the behavior of many stacks over 20 min. Therefore, we have analyzed the timing of events in the different categories (Figure 5B–5D). No specific preference for *trans* first or *trans* last events was detectable in any of the datasets. The average start time of events in each category ranged from 7 to 13 min and none of the categories clearly preceded the others (Figure 5B and 5C). This suggests that, within the first 20 min of treatment, there is no preferential order of fusion.

DISCUSSION

Among eukaryotic organelles, the Golgi apparatus has attracted considerable attention because of its unusual three-dimensional organization and remarkable dynamic behavior, both of which have defied simple explanations. Despite

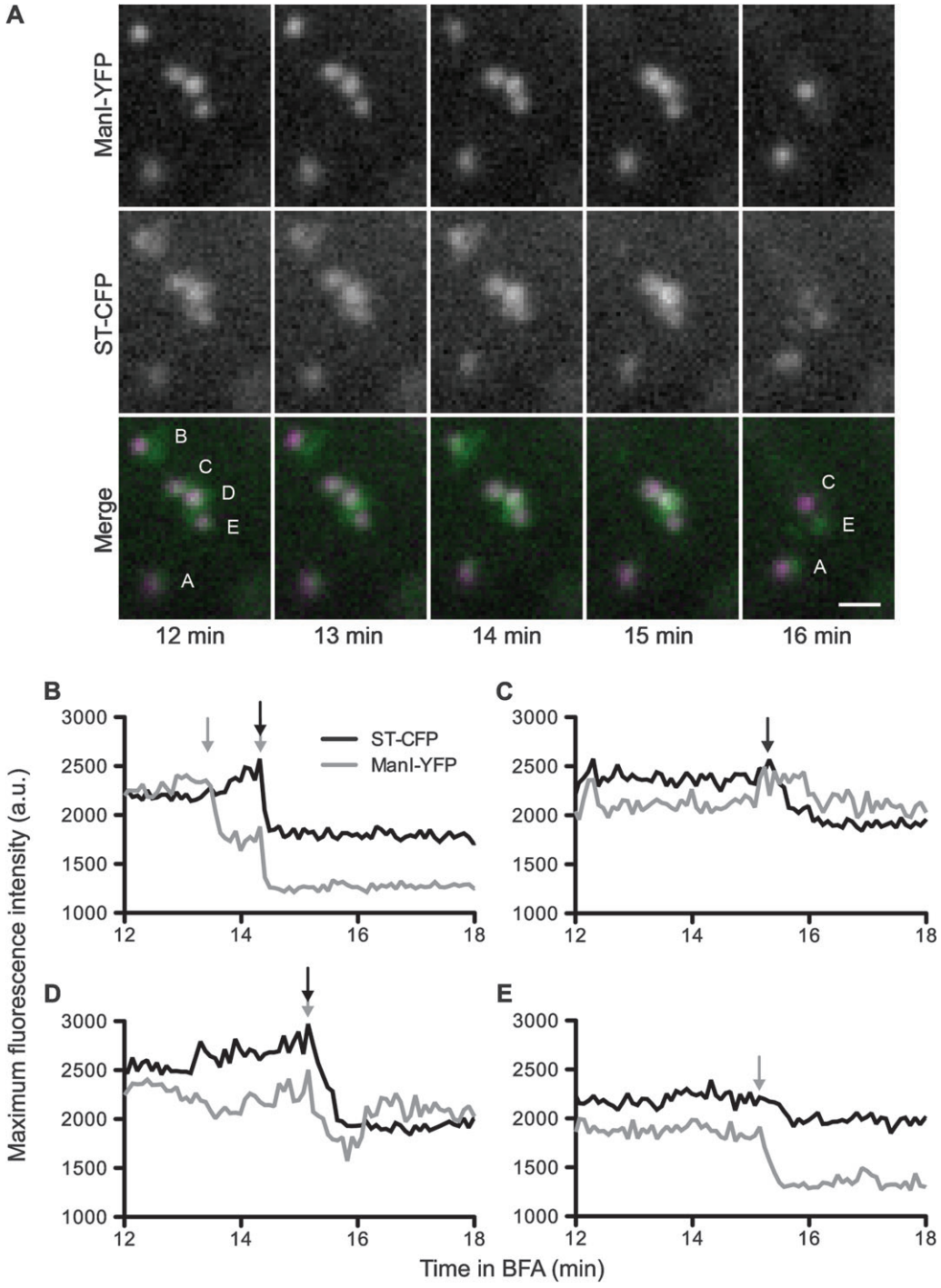

Figure 4. Brefeldin A Treatment Can Result in Sequential Loss of ST–CFP and ManI–YFP.

(A) Five Golgi stacks from a transgenic tobacco BY-2 cell co-expressing ST–CFP (green) and ManI–YFP (magenta) are shown 12–16 min after the addition of brefeldin A.

(B–E) Maximal fluorescence intensities of individual stacks marked in (A) were plotted as a function of treatment time. Black and gray arrows indicate the start of the decrease in fluorescence intensity for ST–CFP and Man1–YFP, respectively. Note that stacks B and D lost both markers simultaneously, while stack C only lost the *trans* marker and stack E lost only the *cis* marker. Scale bar = 2 μm.

many decades of intensive research, we still have no detailed explanation of the mechanisms that maintain Golgi cisternae in a stable stacked arrangement with a clear *cis*-to-*trans* polarity while at the same time permitting continuous flow of secretory products through the organelle (Schoberer and Strasser, 2011). The plant cell Golgi introduces an additional layer of complexity

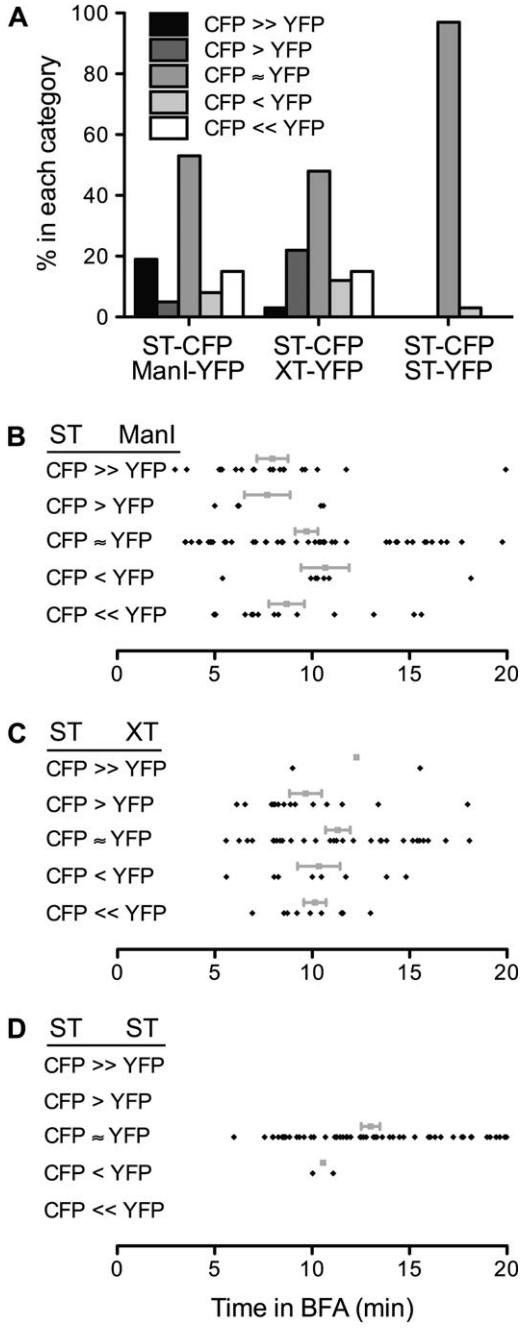

Figure 5. Golgi Disassembly Can Occur in Either a *Trans*-to-*Cis* or a *Cis*-to-*Trans* Direction.

Transgenic tobacco BY-2 cells co-expressing ST–CFP and ManI–YFP **(A, B)**, XT–YFP (A, **C**), or ST–YFP (A, **D**) were treated with brefeldin A and observed for 20 min. Individual stacks could have lost both markers within 10 s of each other (CFP ≈ YFP), within 10–30 s of each other (CFP > YFP, CFP < YFP), or more than 30 s apart from each other (CFP » YFP, CFP « YFP). Gray squares shown in (B–D) represent the average ± the standard error of the mean. Note that about half of the events affected the two markers independently when they localized to different cisternae (A). There was no apparent preference in timing for simultaneous or sequential events for any of the marker combinations (B–D).

by displaying rapid stop and go movements that put additional requirements on Golgi stack coherence and vesicle targeting (Nebenführ and Staehelin, 2001). In this study, we utilized detailed time-lapse observations of dual-labeled Golgi stacks to investigate various aspects of Golgi stack dynamics and integrity.

Different sub-compartments of the Golgi were labeled with fluorescent protein fusions to different Golgi-targeting domains. The transmembrane domains of mannosidase I (ManI), xylosyltransferase (XT), and sialyltransferase (ST) fused to fluorescent proteins have already been shown by immunogold labeling to localize primarily to the *cis*, medial, and *trans* cisternae, respectively (Boevink et al., 1998; Nebenführ et al., 1999; Pagny et al., 2003; Saint-Jore-Dupas et al., 2006). When ST–CFP and ST–YFP were co-expressed, their signals almost completely overlapped. The slight differences of ST–CFP and ST–YFP fluorescence signals may have resulted from the use of sequential time-lapse imaging, which has a delay between the capture of CFP and YFP images. During this delay, the Golgi stacks could have shifted slightly. Importantly, the differences between ST–CFP and ST–YFP signals were always smaller than the differences observed with other marker pairs.

Confirming previous findings from confocal microscopy, we observed with wide-field epifluorescence that ST–CFP fluorescence did not completely overlap with ManI–YFP or XT–YFP fluorescence, indicating that the fusion proteins are localized to different compartments (Boevink et al., 1998; Nebenführ et al., 1999; Pagny et al., 2003; Saint-Jore-Dupas et al., 2006). Similar results have been obtained previously with combinations of other Golgi markers in tobacco leaf epidermal cells (Saint-Jore-Dupas et al., 2006; Latijnhouwers et al., 2007; Schoberer et al., 2010). Thus, it is possible to distinguish different sub-compartments of the Golgi based on the slight separation of signal distributions of the two fluorophores with wide-field epifluorescence microscopy, even though the small size of Golgi stacks (cisternal diameter ~800 nm, stack thickness ~300 nm) is just slightly over the theoretical resolution limit of visible light microscopy (200–350 nm). The different localization of the two markers was most easily seen when observing side-views of Golgi stacks. We cannot determine whether or not the markers label a single cisterna or several; however, previous immunogold labeling suggests that the markers probably label two or more cisternae (Boevink et al., 1998; Nebenführ et al., 1999; Pagny et al., 2003). Interestingly, ManI–YFP often formed smaller fluorescent spots than the other markers, which is consistent with the observations of a smaller diameter of *cis* cisternae in EM images (Staehelin and Kang, 2008). In summary, the employed markers localize to different sub-compartments of the Golgi, thus allowing us to observe the fate of these different cisternae in living cells.

Monensin Preferentially Affects the *Trans* Cisternae

Using electron microscopy, monensin has been shown to lead to swelling of the *trans*-Golgi network, followed by similar effects on the *trans* cisternae and eventually also on the medial and *cis* cisternae (Zhang et al., 1992). This effect has been

interpreted as resulting from an exchange of K^+ ions and protons across the Golgi membranes, hence the stronger effect in the more acidic late Golgi compartments (Zhang et al., 1992; Satiat-Jeunemaitre et al., 1994). We could confirm these findings by using live-cell imaging to compare the rate of swelling between ST–CFP-labeled cisternae and either ManI–YFP or XT–YFP-labeled cisternae. In both cases, the *trans* cisternae swelled to a greater extent compared to the medial and *cis* cisternae. Frequently, we observed *trans* cisternae from different stacks come in close proximity to each other while the other end of the stacks were pointed away from the cluster. This has not been described before, possibly because such larger-scale rearrangements are difficult to discern in EM thin sections. Alternatively, it is also possible that the clustering effect does not occur in sycamore cells (Zhang et al., 1992; Satiat-Jeunemaitre et al., 1994) but is specific for BY-2 cells. We also occasionally observed an increase in fluorescence intensity that coincided with the cisternal swelling. When observed, the increase in fluorescence intensity was usually greater for the ST–CFP marker (data not shown). This is consistent with the predicted alkalinization effect of monensin on the lumen of Golgi cisternae (Pressman and Fahim, 1982), since fluorescent proteins have reduced fluorescence efficiency at low pH (Tamura et al., 2003).

Golgi Stacks Move as Intact Units with Various Orientations

We used simultaneous imaging of CFP and YFP fluorescence to investigate the orientation and integrity of Golgi stacks while they were moving through the cell. Because of this unique approach, we were able to directly determine the location of each marker at any given moment in order to calculate the distance between *cis* and *trans* cisternae. We did not observe any Golgi stacks with a distance larger than 0.8 μm between the centers of ST–CFP and ManI–YFP signals, even when stacks were moving with speeds of up to 3 μm s^{-1}. This suggests that Golgi stacks remain intact while traveling through the cytoplasm. While this has been expected based on the scarcity of stack fragments in electron micrographs, this has not been documented before experimentally.

The observed separation of *cis* and *trans* markers could, in principle, result from two different effects. On the one hand, Golgi cisternae may have shifted relative to each other, as in a slanted stack of books, such that the front-most cisterna is traveling ahead of the trailing cisterna. For the vast majority of the observed Golgi stacks, this would imply that the *trans* cisternae were displaced relative to the *cis* cisternae by less than one half of their diameter. Such 'sheared' Golgi stacks are sometimes visible in EM images, although the separation of *cis* and *trans* cisternae may not be as large as the maximum described here (Nebenführ, unpublished observations). On the other hand, Golgi stacks might move perpendicular to the plane of the cisternae. In this case, the separation of the signals would simply represent the distance between *cis* and *trans* cisternae within a stack. Previously, it was suggested that Golgi stack movements preferentially occurred in the plane of the cisternae (Nebenführ et al., 1999), which would rule out the second option. Our images, unfortunately, do not allow us to distinguish between these possibilities, since the relatively long exposure time needed to collect sufficient signal from both fluorophores (500 ms) results in a slight stretching of the shape of the fluorescent spots in the direction of movement. Alternative imaging approaches with higher temporal and spatial resolution will be necessary to resolve this issue.

Previous findings indicated that Golgi stack movements rely on the acto-myosin network (Boevink et al., 1998; Nebenführ et al., 1999). Recently, T-DNA knockout mutants for various class XI myosin isoforms in *Arabidopsis thaliana* supported the involvement of myosin motors, since several single, double, triple, and quadruple mutants showed reduced Golgi stack motility (Peremyslov et al., 2008; Prokhnevsky et al., 2008; Peremyslov et al., 2010). Similarly, overexpression of dominant-negative myosin tail fragments slowed down Golgi stack movements in tobacco leaf epidermal cells (Avisar et al., 2008; Sparkes et al., 2008; Avisar et al., 2009). These results do not establish, however, whether Golgi stacks are moved directly by myosin motors attached to their surface, or whether their movement depends on association with another motile organelle such as the ER. Such an association was proposed when it became evident that Golgi stacks remain in close association with ER export sites (ERES) that were labeled with components of the COPII machinery. More recently, a physical connection between Golgi stacks and ER membranes was supported with results from laser trap experiments (Sparkes et al., 2009). On the other hand, direct binding of myosins to the plant Golgi has been suggested by labeling of stacks with fragments of a myosin organelle-binding domain (Li and Nebenführ, 2007).

The observation that either end of a Golgi stack can move ahead of the other may provide insights into this question of direct versus indirect Golgi propulsion. In particular, it can be expected that the part of the Golgi where a force is applied should move ahead while the other end of the Golgi will be dragged behind. The fact that we have observed both kinds of Golgi stack movements, *cis* side leading or *trans* side leading, is difficult to reconcile with the ERES attachment model that presumably should result in a more uniform orientation, with the *cis* cisternae leading. Direct attachment of myosin motors to all sides of the Golgi, on the other hand, could explain the observations presented here. In many cases, a moving Golgi stack kept alternating between having the *trans* and *cis* cisternae lead. These alternating polarities could be explained by a continuous change in orientation as a Golgi stack 'rolls' along the actin filament with the aid of multiple motor proteins bound all over its surface. It is also conceivable that the seemingly continuous movements observed by us in 1-s intervals actually consisted of a series of short runs interrupted by release of the actin filament from the Golgi myosin and rebinding on a different surface of the stack. Overall, we did observe a slight bias for the *cis* end of the Golgi stack to lead during movements. This may suggest that the *cis* side of Golgi stacks carries

a higher density of myosin motor proteins or that the myosin motors on that half of the Golgi are more active. Further research will be needed to test this hypothesis; in particular, identification of Golgi myosins and their distribution on the Golgi surface will be crucial.

Golgi Stack Disassembly Can Occur in Either the *Trans*-to-*Cis* or *Cis*-to-*Trans* Direction

Previous studies have shown that brefeldin A (BFA) treatment results in the redistribution of Golgi enzymes to the endoplasmic reticulum (ER; Boevink et al., 1998; Ritzenthaler et al., 2002; Saint-Jore et al., 2002; Schoberer et al., 2010). Normal retrograde transport from the Golgi back to the ER requires COPI-coated vesicles (Letourneur et al., 1994). COPI coat proteins, however, are no longer recruited to Golgi stack membranes when plant cells are treated with BFA (Ritzenthaler et al., 2002), consistent with a BFA-induced block of ARF activation by Sec7-type ARF–GEFs (Donaldson et al., 1992). It has been proposed that the resulting redistribution of Golgi proteins to the ER during BFA treatment is a result of Golgi and ER membrane fusion in the absence of vesicle formation (Elazar et al., 1994; Nebenführ et al., 2002). An alternative model postulates that BFA unmasks a COPI-independent retrograde transport pathway of Golgi enzymes into the ER (e.g. Schoberer et al., 2010). Furthermore, two independent studies concluded that Golgi enzyme redistribution into the ER occurs sequentially in a *trans*-to-*cis* direction (Ritzenthaler et al., 2002; Schoberer et al., 2010).

To further identify the events and possible mechanisms of BFA-induced Golgi stack disassembly, we performed detailed time-lapse imaging of cells co-expressing ST–CFP and ManI–YFP, ST–CFP and XT–YFP, or ST–CFP and ST–YFP during the first 20 min of BFA treatment. The short interval between individual time-lapse images (5 s) allowed us to precisely determine the time at which the fluorescence signal was lost from a Golgi stack as well as the time it took for the fluorescence intensity to reach background levels (typically 15–20 s). The duration of loss of fluorescence signal from individual Golgi stacks in BFA-treated cells was significantly shorter than expected from the normal half-life of Golgi residents measured in FRAP experiments (2–5 min; Brandizzi et al., 2002; Schoberer et al., 2010). This suggests that loss of a Golgi marker into the ER in response to BFA involves processes that do not normally operate in an untreated cell (Sciaky et al., 1997). Thus, we interpret the loss of fluorescence signal from a stack as indicating a BFA-induced fusion of the labeled cisternae with the ER (Ritzenthaler et al., 2002).

In almost all of the cases in which ST–CFP and ST–YFP were co-expressed, both markers were lost simultaneously. This result supports the idea that proteins localized to the same cisternae will redistribute to the ER simultaneously following treatment with BFA. On the other hand, when either *cis* and *trans* markers or medial and *trans* markers were co-expressed, about half of the stacks observed lost their fluorescence signals sequentially. This is consistent with the sequential fusion of cisternae with the ER that has been described by Ritzenthaler et al. (2002) based on EM images. It should be noted that the large number of Golgi stacks that lost both fluorescent signals at the same time would not have been detected in the previous study.

Our finding of a random order of fusion for *cis* and *trans* cisternae, on the other hand, contradicts conclusions that BFA-induced Golgi stack disassembly always occurs in the *trans*-to-*cis* direction (Ritzenthaler et al., 2002; Schoberer et al., 2010). Apparently, the interpretation of the EM images as representing *cis* cisternae (Ritzenthaler et al., 2002) was incorrect and we now assume that about half of the Golgi stack remnants in our earlier study actually represented the *trans* half. It is unclear why the recent study by Schoberer et al. (2010) did not observe the same random distribution of ER–Golgi fusions as described here. In that case, both Golgi membrane proteins and Golgi matrix markers residing in the *trans* half of the stacks were found to be preferentially lost during BFA treatments of tobacco leaf epidermis cells (Schoberer et al., 2010). It is possible that this reflects tissue-specific differences between suspension-cultured BY-2 cells, which have been proposed to be derived from root cells (Winicur et al., 1998), and leaf epidermis cells (Robinson et al., 2008).

Our results indicate that, following BFA treatment, fusion between ER and Golgi membranes can occur anywhere on the Golgi stack. We postulate that the order of cisternal fusion with the ER is determined by the relative proximity of the different cisternae to the ER, such that the cisterna closest to the ER will be the first to fuse with it. This fusion may then lead to a disruption of normal Golgi organization, which results in additional fusion events with the remaining cisternae. Consistent with this model, we observed that the delay between *trans* and medial fusion events tended to be shorter than the delay between *trans* and *cis* fusions.

Drug Treatments as Useful Tools for Protein Localization within the Golgi

Identification of the precise sub-Golgi localization of a given protein is of great interest, since cargo molecules traverse the cisternae in a predictable *cis*-to-*trans* direction and therefore encounter Golgi-resident enzymes in a particular order. This is already well established for enzymes involved in the modification of N-linked oligosaccharides that are arranged in an assembly-line fashion according to the order in which they operate on their substrates (reviewed in Schoberer and Strasser, 2011). Enzymes involved in the synthesis of cell wall polysaccharides presumably also follow a similar arrangement (Zhang and Staehelin, 1992). However, very little is currently known about their distribution in Golgi stacks (Chevalier et al., 2010).

The most commonly used technique for determining the localization of proteins within the Golgi is using immunogold labeling and electron microscopy (e.g. Saint-Jore-Dupas et al., 2006; Chevalier et al., 2010). While providing the most definitive evidence for cisternal localization, this method is technically challenging and requires suitable antibodies that recognize their epitope in fixed and embedded material. The results presented here, on the other hand, suggest that

a relatively simple approach based on three fluorescently labeled markers and two drug treatments can give a good indication as to which section of a Golgi stack (*cis*, medial, or *trans*) the protein resides in. For example, the protein of interest fused to CFP could be co-expressed in tobacco BY-2 cells with ManI–YFP, XT–YFP, or ST–YFP. Researchers can then compare the localization of their protein to these three standard markers as well as perform BFA and monensin experiments to further confirm the location of the protein within the Golgi. An even simpler 'first-look' experiment might involve only co-expression with a medial marker such as XT–YFP followed by BFA and monensin treatments. Simultaneous loss of CFP and YFP signals in BFA would be interpreted as medial localization of the protein of interest. Sequential loss of signals would suggest *cis* or *trans* localization, which would be easily resolved with monensin treatment. Thus, our observations suggest a simple procedure for the identification of the localization of unknown membrane proteins to specific Golgi sub-compartments.

CONCLUSIONS

Golgi stacks display a remarkable stability during rapid intracellular movements, which is probably due to the action of matrix proteins that anchor the cisternae to each other. Although Golgi stacks display a clear *cis*-to-*trans* polarity that is reflected in both cisternal morphology and protein composition, there is little to no difference between cisternae when it comes to myosin-driven movements or BFA responses. The specialization of different cisternae, on the other hand, is detectable by monensin treatment, which presumably is reflective of the higher luminal acidity in *trans* cisternae. We speculate that myosin motor proteins are binding all over the surface of Golgi stacks, which allows them to move in any direction and even change their orientation during movements along actin filaments. Finally, we demonstrate that a combination of Golgi markers with known localization and drug treatments is sufficient to predict the sub-Golgi localization of unknown membrane proteins by fluorescence microscopy.

METHODS

Materials

Tobacco (*Nicotiana tabacum* var. Bright Yellow 2) cells were grown in modified Murashige and Skoog medium under constant shaking (120 rpm) in the dark at 27°C (Nagata et al., 1982). The cells were transferred to fresh medium every week using a 1:200 dilution to maintain them in the log growth phase. Each cell line was transformed with two of the following markers: (1) soybean α-1,2 mannosidase I–YFP, which localizes predominately to the *cis* end of the Golgi (Nebenführ et al., 1999; Saint-Jore-Dupas et al., 2006), (2) *Arabidopsis thaliana* β1,2-xylosyltransferase–YFP, which is used to label medial cisternae (Pagny et al., 2003), and (3) rat α-2,6-sialyltransferase–YFP (or CFP), which primarily localizes to the *trans* half of the Golgi (Boevink et al., 1998). The *cis* marker is based on the full-length protein (Nebenführ et al., 1999). For the medial marker, the coding region corresponding to the first 36 amino acids of XT was amplified from *Arabidopsis* cDNA. The *trans* markers incorporate the first 52 amino acids of ST and was a kind gift by Dr Chris Hawes (Oxford Brookes University, UK). All markers carry the fluorescent protein at their C-termini in the lumen of the Golgi. Expression of all markers was driven by the double 35S promoter (Nelson et al., 2007). The expression constructs were cloned into binary plasmids (pVKH18, pFGC19, pBIN20) and transformed via *Agrobacterium* into BY-2 cells as described previously (Nebenführ et al., 1999). Selection of transformed cells was achieved by adding 100 μg ml^{-1} hygromycin, 10 μg ml^{-1} glufosinate, or 50 μg ml^{-1} kanamycin, respectively, to the medium.

Microscopy

Tobacco BY-2 cells co-expressing two fluorescent protein fusions were visualized using an Axiovert 200 M microscope (Zeiss) equipped with filters for CFP and YFP fluorescence (C-35520; Chroma Technology). Transgenic cells were observed in their cortical cytoplasm closest to the cover slip with a 63× (1.4 NA) plan-apo oil immersion objective, and images were captured using a digital camera (Orca ER; Hamamatsu Photonics) using OpenLab5 software (Improvision/Perkin Elmer). Most CFP and YFP images were taken sequentially after switching the excitation light with an external DG-4 wavelength switcher (Sutter Instruments). For simultaneous image capture, the excitation wavelengths were rapidly alternated (CFP/YFP/CFP/YFP/CFP) during a single exposure to avoid sequential detection of the two markers. In this case, an image splitter (Dual-View; Optical Insights) was used to separate the emission wavelengths into two images that were projected side by side on the camera chip (dichroic filter 505dcxr; emission filters D465/30 for CFP and HQ535/30 for YFP; Chroma Technology). The CFP and YFP half-images were separated and CFP bleed-through was removed computationally from the YFP image. For all images, background subtraction was used to remove camera noise prior to quantitative analysis. Contrast enhancement was used to increase the signal intensity and decrease background fluorescence for presentation in the figures and supplemental movies. To determine the relative position of two cisternae in the same Golgi stack, a peak-finding plug-in (Particle Tracker; http://weeman.inf.ethz.ch/particletracker; Sabalzarini and Koumoutsakos, 2005) to ImageJ (http://rsb.info.nih.gov/ij/) was used.

Monensin Treatment

Three to 5-day-old tobacco BY-2 cells were placed in a perfusion chamber and modified Murashige and Skoog medium was perfused at 0.5 ml min^{-1}. Sequential time-lapse imaging was started about 3 min before monensin (Acros Chemicals) and latrunculin B (LatB) were added. Images were taken for 60 min with 10-s intervals using CFP and YFP filters. Final monensin concentration was 10 μM from a stock solution of 3 mM

in ethanol, and LatB had a final concentration of 1 μM from a stock solution of 1 mM in DMSO. Sizes of cisternae were measured in ImageJ after manual selection of the fluorescent areas.

Movement Analysis

Six-day-old tobacco BY-2 cells co-expressing ST–CFP and ManI–YFP were observed. Simultaneous image capture was used to capture time-lapse images in 1-s intervals over 1 min. After separation of the CFP and YFP signals, 20 individual Golgi stacks were traced over time separately in the CFP and YFP images using OpenLab5 software. X and Y coordinates of the manually selected center points were transformed so that the direction of movement was in the positive X direction, with very little movement in the Y direction. This allowed for progress of the stacks to be followed along this new axis with the new parameter *d*. For each time point, the location of the stack in the YFP image was subtracted from its location in the CFP image to obtain the distance between the *cis* and *trans* cisternae ($d_{CFP} - d_{YFP}$). Thus, positive values indicate the *trans* cisternae leading, whereas negative values indicate the *cis* cisternae leading. Neither half was considered to be leading when the measured distance between the ST–CFP and ManI–YFP markers was less than 0.14 μm, which is less than half the length of the diagonal of a pixel. For every image, the speed in each frame was calculated by OpenLab5 software. The calculated CFP and YFP image speeds were averaged to obtain the overall speed of the Golgi stack at that time point.

Brefeldin A Treatment

Three to 6-day-old tobacco BY-2 cells were treated with brefeldin A (BFA, Molecular Probes/Invitrogen) and latrunculin B (LatB, Sigma) while on a large coverslip on the inverted microscope. BFA was used at a final concentration of 10 μg ml^{-1} from a stock solution of 5 mg ml^{-1} in ethanol. LatB had a final concentration of 1 μM. Cells were observed for 20 min after drugs were added by sequential time-lapse imaging with 5-s intervals between images. Individual Golgi stacks were identified manually, and OpenLab5 software was used to measure the maximal fluorescence intensities of the selected areas for every frame in the image sequence.

SUPPLEMENTARY DATA

Supplementary Data are available at *Molecular Plant Online.*

FUNDING

Work in our lab is supported by the National Science Foundation (grant MCB-0822111 to A.N.).

ACKNOWLEDGMENTS

We thank Dr Xue Cai for the assembly of the ManI–YFP, ST–YFP, and ST–CFP expression constructs. The original ST–GFP plasmid was a kind gift from Dr Chris Hawes (Oxford Brookes University, UK). We thank Dr Krzysztof Bobik and Jennifer M. Ryan for critical reading of the manuscript. No conflict of interest declared.

REFERENCES

Avisar, D., Abu-Abied, M., Belausov, E., Sadot, E., Hawes, C., and Sparkes, I.A. (2009). A comparative study of the involvement of 17 *Arabidopsis* myosin family members on the motility of Golgi and other organelles. Plant Physiol. **150,** 700–709.

Avisar, D., Prokhnevsky, A.I., Makarova, K.S., Koonin, E.V., and Dolja, V.V. (2008). Myosin XI-K is required for rapid trafficking of Golgi stacks, peroxisomes, and mitochondria in leaf cells of *Nicotiana benthamiana*. Plant Physiol. **146,** 1098–1108.

Boevink, P., Oparka, K., Sant Cruz, S., Martin, B., Betteridge, A., and Hawes, C. (1998). Stacks on tracks: the plant Golgi apparatus traffics on an actin/ER network. Plant J. **15,** 441–447.

Boss, W.F., Morre, D.J., and Mollenhauer, H.H. (1984). Monensin-induced swelling of Golgi apparatus cisternae mediated by a proton gradient. Eur. J. Cell Biol. **34,** 1–8.

Brandizzi, F., Snapp, E., Roberts, A., Lippincott-Schwartz, J., and Hawes, C. (2002). Membrane protein transport between the ER and Golgi in tobacco leaves is energy dependent but cytoskeleton independent: evidence from selective photobleaching. Plant Cell. **14,** 1293–1309.

Chevalier, L., et al. (2010). Subcompartment localization of the side chain xyloglucan-synthesizing enzymes within Golgi stacks of tobacco suspension-cultured cells. Plant J. **64,** 977–989.

de Graffenried, C.L., and Bertozzi, C.R. (2004). The roles of enzyme localisation and complex formation in glycan assembly within the Golgi apparatus. Curr. Opin. Cell Biol. **16,** 356–363.

Donaldson, J.G., Finazzi, D., and Klausner, R.D. (1992). Brefeldin A inhibits Golgi-membrane catalysed exchange of guanine nucleotide onto ARF protein. Nature. **360,** 350–352.

Driouich, A., Faye, L., and Staehelin, L.A. (1993). The plant Golgi apparatus: a factory for complex polysaccharides and glycoproteins. Trends Biochem. Sci. **18,** 210–214.

Elazar, Z., Orci, L., Ostermann, J., Amherdt, M., Tanigawa, G., and Rothman, J.E. (1994). ADP-ribosylation factor and coatomer couple fusion to vesicle budding. J. Cell Biol. **124,** 415–424.

Jiang, L., and Rogers, J.C. (1999). Functional analysis of a Golgi-localized Kex2p-like protease in tobacco suspension culture cells. Plant J. **18,** 23–32.

Latijnhouwers, M., Gillespie, T., Boevink, P., Kriechbaumer, V., Hawes, C., and Carvalho, C.M. (2007). Localization and domain characterization of *Arabidopsis* golgin candidates. J Exp. Bot. **58,** 4373–4386.

Latijnhouwers, M., Hawes, C., and Carvalho, C. (2005). Holding it all together? Candidate proteins for the plant Golgi matrix. Curr. Opin. Plant Biol. **8,** 632–639.

Lee, M.H., et al. (2002). ADP-ribosylation factor 1 of *Arabidopsis* plays a critical role in intracellular trafficking and maintenance of endoplasmic reticulum morphology in *Arabidopsis*. Plant Physiol. **129,** 1507–1520.

Letourneur, F., et al. (1994). Coatomer is essential for retrieval of dilysine-tagged proteins to the endoplasmic reticulum. Cell. **79,** 1199–1207.

Li, J.-F., and Nebenführ, A. (2007). Organelle targeting of myosin XI is mediated independently by two globular tail subdomains. J. Biol. Chem. **282,** 20593–20602.

Matheson, L.A., et al. (2007). Multiple roles of ADP-ribosylation factor 1 in plant cells include spatially regulated recruitment of coatomer and elements of the Golgi matrix. Plant Physiol. **143,** 1615–1627.

Nagata, T., Nemoto, Y., and Hasezawa, S. (1982). Tobacco BY-2 cell line as the 'HeLa' cell in the cell biology of higher plants. International Review of Cytology. **132,** 1–30.

Nebenführ, A. (2003). Intra-Golgi transport: escalator or bucket brigade? In The Golgi Apparatus and the Plant Secretory Pathway Robinson, D.G., ed. (Oxford: Blackwell). pp. 76–89.

Nebenführ, A., and Staehelin, L.A. (2001). Mobile factories: Golgi dynamics in plant cells. Trends Plant Sci. **6,** 160–167.

Nebenführ, A., et al. (1999). Stop-and-go movements of plant Golgi stacks are mediated by the acto-myosin system. Plant Physiol. **121,** 1127–1141.

Nebenführ, A., Ritzenthaler, C., and Robinson, D.G. (2002). Brefeldin A: deciphering an enigmatic inhibitor of secretion. Plant Physiol. **130,** 1102–1108.

Nelson, B.K., Cai, X., and Nebenführ, A. (2007). A multi-color set of *in vivo* organelle markers for colocalization studies in *Arabidopsis* and other plants. Plant J. **51,** 1126–1136.

Osterrieder, A., Hummel, E., Carvalho, C.M., and Hawes, C. (2010). Golgi membrane dynamics after induction of a dominant-negative mutant Sar1 GTPase in tobacco. J Exp Bot. **61,** 405–422.

Pagny, S., et al. (2003). Structural requirements for *Arabidopsis* beta1,2-xylosyltransferase activity and targeting to the Golgi. Plant J. **33,** 189–203.

Peremyslov, V.V., Prokhnevsky, A.I., Avisar, D., and Dolja, V.V. (2008). Two class XI myosins function in organelle trafficking and root hair development in *Arabidopsis thaliana*. Plant Physiol. **146,** 1109–1116.

Peremyslov, V.V., Prokhnevsky, A.I., and Dolja, V.V. (2010). Class XI myosins are required for development, cell expansion, and F-Actin organization in *Arabidopsis*. Plant Cell. **22,** 1883–1897.

Polishchuk, R.S., and Mironov, A.A. (2004). Structural aspects of Golgi function. Cell Mol. Life Sci. **61,** 146–158.

Pressman, B.C., and Fahim, M. (1982). Pharmacology and toxicology of the monovalent carboxylic ionophores. Annu. Rev. Pharmacol. Toxicol. **22,** 465–490.

Prokhnevsky, A.I., Peremyslov, V.V., and Dolja, V.V. (2008). Overlapping functions of the four class XI myosins in *Arabidopsis* growth, root hair elongation, and organelle motility. Proc. Natl. Acad. Sci. U S A **105,** 19744–19749.

Renna, L., Hanton, S.L., Stefano, G., Bortolotti, L., Misra, V., and Brandizzi, F. (2005). Identification and characterization of AtCASP, a plant transmembrane Golgi matrix protein. Plant Mol. Biol. **58,** 109–122.

Ritzenthaler, C., et al. (2002). Reevaluation of the effects of brefeldin A on plant cells using tobacco bright yellow 2 cells expressing Golgi-targeted green fluorescent protein and COPI antisera. Plant Cell. **14,** 237–261.

Robinson, D.G., Langhans, M., Saint-Jore-Dupas, C., and Hawes, C. (2008). BFA effects are tissue and not just plant specific. Trends Plant Sci. **13,** 405–408.

Runions, J., Brach, T., Kuhner, S., and Hawes, C. (2006). Photoactivation of GFP reveals protein dynamics within the endoplasmic reticulum membrane. J Exp. Bot. **57,** 43–50.

Sabalzarini, I.F., and Koumoutsakos, P. (2005). Feature point tracking and trajectory analysis for video imaging in cell biology. J. Struc. Biol. **151,** 182–195.

Saint-Jore, C.M., Evins, J., Batoko, H., Brandizzi, F., Moore, I., and Hawes, C. (2002). Redistribution of membrane proteins between the Golgi apparatus and endoplasmic reticulum in plants is reversible and not dependent on cytoskeletal networks. Plant J. **29,** 661–678.

Saint-Jore-Dupas, C., et al. (2006). Plant N-glycan processing enzymes employ different targeting mechanisms for their spatial arrangement along the secretory pathway. Plant Cell. **18,** 3182–3200.

Satiat-Jeunemaitre, B., et al. (1994). Differential effects of monensin on the plant secretory pathway. J. Exp. Bot. **45,** 685–698.

Schoberer, J., and Strasser, R. (2011). Sub-compartmental organization of Golgi-resident N-glycan processing enzymes in plants. Mol. Plant. **4,** 220–228.

Schoberer, J., Runions, J., Steinkellner, H., Strasser, R., Hawes, C., and Osterrieder, A. (2010). Sequential depletion and acquisition of proteins during Golgi stack disassembly and reformation. Traffic. **11,** 1429–1444.

Sciaky, N., et al. (1997). Golgi tubule traffic and the effects of brefeldin A visualized in living cells. J. Cell Biol. **139,** 1137–1155.

Sparkes, I.A., Ketelaar, T., de Ruijter, N.C.A., and Hawes, C. (2009). Grab a Golgi: laser trapping of Golgi bodies reveals *in vivo* interactions with the endoplasmic reticulum. Traffic. **10,** 567–571.

Sparkes, I.A., Teanby, N.A., and Hawes, C. (2008). Truncated myosin XI tail fusions inhibit peroxisome, Golgi, and mitochondrial movement in tobacco leaf epidermal cells: a genetic tool for the next generation. J. Exp. Bot. **59,** 2499–2512.

Staehelin, L.A., and Kang, B.H. (2008). Nanoscale architecture of endoplasmic reticulum export sites and of Golgi membranes as determined by electron tomography. Plant Physiol. **147,** 1454–1468.

Staehelin, L.A., and Moore, I. (1995). The plant Golgi apparatus: structure, functional organization and trafficking mechanisms. Ann. Rev. Plant Physiol. Plant. Mol. Biol. **46,** 261–288.

Tamura, K., et al. (2003). Why green fluorescent fusion proteins have not been observed in the vacuoles of higher plants. Plant J. **35,** 545–555.

Ueda, H., et al. (2010). Myosin-dependent endoplasmic reticulum motility and F-actin organization in plant cells. Proc. Natl Acad. Sci. U S A. **107,** 6894–6899.

Winicur, Z.M., Zhang, G.F., and Staehelin, L.A. (1998). Auxin deprivation induces synchronous Golgi differentiation in suspension-cultured tobacco BY-2 cells. Plant Physiol. **117,** 501–513.

Zhang, G.F., Driouich, A., and Staehelin, L.A. (1993). Effect of monensin on plant Golgi: re-examination of the monensin-induced swelling in cisternal architecture and functional activities of the Golgi apparatus of sycamore suspension-cultured cells. J. Cell Sci. **104,** 819–831.

Zhang, G.F., and Staehelin, L.A. (1992). Functional compartmentation of the Golgi apparatus of plant cells: immunocytochemical analysis of high-pressure frozen- and freeze-substituted sycamore maple suspension culture cells. Plant Physiol. **99,** 1070–1083.